Biointerface Research in Applied Chemistry
Open-Access Journal (ISSN: 2069-5837)

Article
Volume 13, Issue 5, 2023, 427
https://doi.org/10.33263/BRIAC135.427

Inhibitive Properties of Date Seed Extracts (Phoenix Dactylifera L.) on Mild Steel Corrosion in 1M HCl Solution: Experimental and DFT Studies

Meryem Hrimla [1,*], Abderrahim Alahyane [2], Ali Oubella [3], Lahoucine Bahsis [1,4], Jamal Ayour [2], Imane Elateri [2], Mohamed Abderrazik [2], Hafid Anane [1], My Rachid Laamari [1,*]

1 Laboratory of Analytical and Molecular Chemistry /LCAM, Cadi Ayyad University, Polydisciplinary Faculty of Safi, Sidi Bouzid. B.P. 4162, 46 000 Safi. Morocco; meryemhrimla.uca@gmail.com (M.H.); bahsis.lahoucine@gmail.com (L.B.); h.anane@uca.ma (H.A.); r.laamari@gmail.com (M.L.);
2 Food Sciences Laboratory, Department of Biology, Faculty of Sciences Semlalia, Cadi Ayyad University, P.O. Box 2390, 40090 Marrakesh, Morocco; ab.alahyane@gmail.com (A.A.); jamal.ayour@ced.uca.ac.ma (J.A.); imane.elateri@yahoo.fr (I.E.); m_abderrazik@yahoo.fr (M.A.);
3 Laboratory of Organic Synthesis and Molecular Physical Chemistry, Department of Chemistry, Faculty of Sciences Semlalia, B.P 2390, Marrakech, 40001, Morocco; oubellaali1@gmail.com (A.O.);
4 Department of Chemistry, Faculty of Science of El Jadida, Université Chouaïb Doukkali, B.P.: 20, El Jadida 24000, Morocco; bahsis.lahoucine@gmail.com (L.B.);
* Correspondence: meryemhrimla.uca@gmail.com (M.H.); r.laamari@gmail.com (M.L.);
Scopus Author ID 57211350593
Received: 15.07.2022; Accepted: 26.08.2022; Published: 15.12.2022

Abstract: Date seeds were subjected to electrochemical analysis to inhibit the corrosion of mild steel in an acidic medium of 1 M HCl. The inhibitor inhibition efficacy was studied by gravimetric spectroscopy, potentiodynamic polarization (PDP), and electrochemical impedance spectroscopy (EIS). The results revealed that oil extracts from date pits functioned as cathodic rather than anodic inhibitors, and the maximum corrosion inhibition efficiencies were obtained with an optimal concentration of 700 ppm—adsorption of these extracts on the mild steel surface followed by the Langmuir isotherm. The SEM and EDX characterization confirms the existence of a protective layer on the metal surface. Quantum chemical calculations using the density functional theory (DFT) method was also performed to understand the inhibition and adsorption behavior of the main constituents of Date Seed extract on the Fe surface.

Keywords: date seeds; oil; *Phoenix Dactylifera* L; corrosion inhibition; mild steel; medium acid; quantum chemical calculations.

1. Introduction

Many industries and machinery are widely based on mild steel. However, acids; for example, hydrochloric acid, used in i) the pickling, ii) industrial acid cleaning, iii) cleaning of oil refinery equipment, iv) oil well acidizing, and v) acid descaling, these processes usually lead to substantial loss of the metal cause its deterioration, it is called corrosion of metals [1,2]. This phenomenon causes huge economic costs; damage to the equipment poses a serious threat to the environment and human health [3,4]. Many commercially available methods and strategies to protect metals against corrosion [5,6]. Using organic corrosion inhibitors is one of the effective corrosion control methods. In the corrosion inhibition field, the effective corrosion inhibitors, synthetic or natural, have an active functional group such as nitro (NO_2), hydroxyl

(OH), and conjugated groups; these specific sites can form a coordinative bond by directing their electron pairs towards the 3d orbital of the iron atom [7,8]. Nevertheless, most synthetic inhibitors are very toxic [9–11], which encourages using natural products that are biodegradable, economically viable, and not dangerous to humans and the environment. In this respect, researchers focused on using green corrosion inhibitors of plant origin because most natural organic compounds are effective and environmentally friendly corrosion inhibitors for metals in acidic environments [12–15]. Extracts from many plants have been tested as acid corrosion inhibitors [16,17]. Umoren *et al*. [18] studied the corrosion inhibition of mild steel in an acid medium using date palm seed extracts; the results indicate that the substances can effectively suppress mild steel corrosion with an inhibition efficiency of 85.8% at 2500 ppm. Another study evaluated the extract of *Schinopsis lorentzii* as a green corrosion inhibitor for low carbon steel in 1M HCl solution with a modest inhibition efficiency of 66% at 2000ppm [19], and the extract functioned as a mild cathodic inhibitor and showed a modest inhibition efficacy of 66% at 2000 ppm. In this work, we introduce novel environmentally friendly products such as "*date seeds*" which have a wide range of biological properties due to their bioactive compounds (polyphenols, flavonoids, and condensed tannins), with the presence and predominance of gallic acid and antioxidant activities [20,21]. These products get carefully distinguished as effective corrosion inhibitors for mild steel in 1M HCl solution at 298K.

2. Materials and Methods

2.1. Materials.

The tests were carried out on mild steel samples with the following composition in percent by weight (%): O: 0.03%, Mn: 0.048%, N: 0.012%, S: 0.012%, C: 0.016%, P: 0.001%, and the balance iron (Fe). The corrosive solution 1M HCl was prepared with an analytical grade of HCl (37% by weight) and deionized water. The extracts were dissolved in an acid solution at 300 to 700 ppm concentrations. Without inhibitors, the solution was taken as a blank for comparison. The volume of electrolytes used was 25 mL in each experiment. Six varieties and clones of date seeds have been subjected to electrochemical studies.

2.2. Weight loss measurements.

Gravimetric tests were performed using the mild steel samples with a size of 2 cm × 2 cm × 0.05 cm. After the exposure time, each specimen was carefully rinsed with double-distilled water and then weighed with an analytical balance (accuracy ±0.1mg).

The inhibition efficiency *(IE%)* was determined using equation (1) [22,23].

$$IE\% = \frac{CR_{\circ} - CR}{CR_{\circ}} \times 100 \quad (1)$$

where CR_o and CR are the corrosion rates in the absence and presence of the inhibitor respectively.

2.3. Electrochemical measurements.

Electrochemical measurements were performed to investigate the inhibitory effect of date seed oil extracts in an acidic medium (1 M HCl) using a three-electrode glass cell

connected to a Voltalab 10 system (PGZ 100 radiometer) controlled by Volta master 4 software. All electrochemical tests were performed at room temperature and repeated three times to ensure the accuracy and reproducibility of the data. The EIS tests were carried out in the frequency variety of 100 kHz to 0.1 Hz according to an AC source with an amplitude of 10 mV. PDP tests were carried out by polarizing the specimen from -800 to -300 mV/SCE. The inhibition efficiency (*IE* %) was calculated by using the equations (2) and (3) [24–26]:

$$IE\% = \frac{R_{pi} - R_p}{R_{pi}} \times 100 \quad (2)$$

where R_p (sum of R_{ct} and R_f) and R_{pi} represent the polarization resistance in inhibited and uninhibited solutions, respectively, here, R_f is the film resistance.

$$IE\% = \frac{I - I_i}{I} \times 100 \quad (3)$$

where I and I_i represent the corrosion current density in the absence and the presence of inhibitors, respectively.

2.4. Quantum chemical calculations.

Quantum chemicals based on DFT calculations have been performed using the Gaussian 09 software at B3LYP/ 6-311G(d,p) theoretical level to investigate the adsorption mechanism of the most abandoned compounds in the prepared Date Seed extracts. The electronic structures and inhibition efficiency of the selected molecules were investigated through different descriptors such as the Lowest Unoccupied Molecular Orbital (E_{LUMO}), Highest Occupied Molecular Orbital (E_{HOMO}), energy ($\Delta E = E_{LUMO} - E_{HOMO}$), electronegativity ($\chi$), dipole moment ($\mu$), softness ($\sigma$), hardness ($\eta$), and the portion of transferred electrons (ΔN). Molecular electrostatic potentials (MEPs) were also performed at the same theoretical level. The values of χ, μ, σ, η, and ΔN were determined using the equations (4), (5), (6), (7). [27,28]:

$$\eta = -\frac{1}{2}(E_{HOMO} - E_{LUMO}) \quad (4)$$

$$x = -\frac{1}{2}(E_{HOMO} + E_{LUMO}) \quad (5)$$

$$\sigma = \frac{1}{\eta} \quad (6)$$

$$\Delta N = \frac{\chi\,\mathrm{Fe} - \chi\mathrm{i}}{2(\eta\mathrm{Fe} + \eta\mathrm{i})} \quad (7)$$

where χ_{Fe}, χ_i, η_{Fe}, and η_i represent the electronegativity and the hardness values of iron and the inhibitors, respectively.

3. Results and Discussion

3.1. Fatty acids content.

The fatty acid (FA) composition is an essential indicator of the nutritional value of the oil. The results of the fatty acid analysis of date seeds, which vary slightly within analyzed date seed varieties and clones, are given in Table 1. The most important acids were oleic C18:1, *Linoleic* C18:2, *Lauric* C12:0, *Palmitic* C16:0, *Myristic* C14:0, and *Stearic* C18:0, which represented together more than 98% of the total fatty acids oil. Devshony *et al*. [29] reported that date seed oil might be classified as Lauric-Oleic Oil, in which the most abundant fatty acid in date oil was oleic acid, with the average amount ranging from 49.49% for the BRR variety to 45.91% for the KBN clone, followed by lauric acid. Al-Shahib and Marshall [30] found that the oleic acid content of cultivars of the date seed oil ranges from 41 to 59%, which could be a good source of C18:1 fatty acid. However, Besbes *et al*. [31] found a lower oleic acid content (41.3–47.7%) in date seed oil extracted from Tunisia cultivars. Our findings indicated that lauric acid was the highest fatty acid among saturated fatty acids in all varieties and clones, agreeing with the findings of Al-Shahib and Marshall [30]; these main saturated fatty acids ranged from 19.03% (KBN clone) and 14,64% (MEL clone). There was not much variation in either palmitic (C16:0, hexadecanoic); or stearic acid (C18:0, octadecanoic) contents.

Table 1. Fatty acids composition of date pits oil.

Fatty acids	C12:0	C14:0	C16:0	C18:0	C18:1	C18:2	C20:0	C18:3	C20:1	C22:0	C22:1
	Lauric Acid (%)	Myristic acid (%)	Palmitic acid (%)	Stearic acid (%)	Oleic acid (%)	Linoleic acid (%)	Arachidic acid (%)	Linolenic acid (%)	Eicosenoic acid (%)	Behenic acid (%)	Erucic acid (%)
LHD	17,36± 0.200b	11,30± 0.200a	10,81± 0.249cd	3,77± 0.149c	47,93± 0.099fgh	6,55± 0.099efg	0,45± 0.049a	0,10± 0.049c	0,34± 0.050a	0,27± 0.050a	ND
HFL	15,37± 0.200def	11,25± 0.150a	11,81± 0.099ab	4,12± 0.200abc	48,33± 0.200def	7,14± 0.100de	0,46± 0.049a	0,09± 0.050c	0,32± 0.050a	0,26± 0.050a	ND
KHL	16,91± 0.199bcd	10,27± 0.200abcd	10,29± 0.250d	3,38± 0.100c	49,10± 0.100bcd	7,68± 0.100d	0,41± 0.100a	0,16± 0.050c	0,36± 0.050a	0,26± 0.050a	0,02± 0.050ab
KBN	19,03± 0.300a	11,14± 0.250ab	10,48± 0.150bcd	3,98± 0.099abc	45,91± 0.150j	7,09± 0.100def	0,51± 0.100a	0,11± 0.050c	0,36± 0.050a	0,32± 0.050a	0,01± 0.050ab
MEL	14,64± 0.100f	10,56± 0.001abcd	11,16± 0.100abcd	3,87± 0.199bc	48,28± 0.100efg	8,39± 0.099b	0,47± 0.049a	0,72± 0.050b	0,38± 0.050a	0,26± 0.050a	0,06± 0.050ab
BRR	15,60± 0.250ef	10,65± 0.100abcd	11,05± 0.250abcd	3,99± 0.099abc	49,49± 0.100b	6,97± 0.099efg	0,49± 0.049a	0,09± 0.050c	0,35± 0.050a	0,30± 0.050a	ND

Values are presented as means ± standard deviation (SD) of three replications. Data in the same column followed by different letters are significantly different from each other according to the LSD test; ND: Non-Detected.

3.2. Corrosion inhibition studies.

3.2.1. Gravimetric measurements.

Table 2 illustrates the gravimetric results of mild steel in uninhibited and inhibited solutions. The results show that the inhibitory action increases with the concentration of the different date seeds oil extracts. This observation might be assigned to the adsorption of components of date seed oil extracts on the interface of the steel/HCl solution.

Table 2. The corrosion parameters obtained from weight loss measurements for mild steel in 1M HCl containing various concentrations of date seeds oil extracts at 298K.

	C_{inh} (ppm)	CR (mg cm^{-2} h^{-1})	Θ	IE_w (%)
Blank	-	0.3857	-	-
KHL	300	0.1689	0.5622	56.22
	500	0.1239	0.6788	67.88
	700	0.0748	0.8061	80.61
BRR	300	0.1462	0.6209	62.09
	500	0.1117	0.7104	71.04
	700	0.0715	0.8146	81.46
HFL	300	0.1582	0.5898	58.98
	500	0.1257	0.6741	67.41
	700	0.0907	0.7648	76.48
MEL	300	0.2097	0.4563	45.63
	500	0.1379	0.6425	64.25
	700	0.0923	0.7607	76.07
LHD	300	0.1768	0.5416	54.16
	500	0.1406	0.6355	63.55
	700	0.1078	0.7205	72.05
KBN	300	0.1761	0.5432	54.34
	500	0.1419	0.6321	63.21
	700	0.1077	0.7208	72.08

3.2.2. Electrochemical Measurements.

3.2.2.1. PDP measurements.

Figure 1 shows mild steel's characteristic potentiodynamic polarization curves in 1M HCl in the absence and presence of the various date seeds oil extracts. The electrochemical parameters obtained from these curves are presented in Table 3. As appeared in Table 3, the addition of the different date seeds oil extracts reduces the density of the corrosion current (Icorr) compared to the blank solution, resulting in the adsorption of the inhibitors on the mild steel surface [32], reaching a maximum value of inhibition efficiency at 700 ppm. However, the concentration of the inhibitors has a small influence on the values of the anodic Tafel constant (βa) and the cathodic Tafel constant (βc), which indicates that the inhibitors act on the mild steel surface without modifying the mechanism of the cathodic reaction and the process of anodic dissolution [33]. Furthermore, the shift of Ecorr to the cathodic direction indicates that the examined additives could be considered cathodic inhibitors [34].

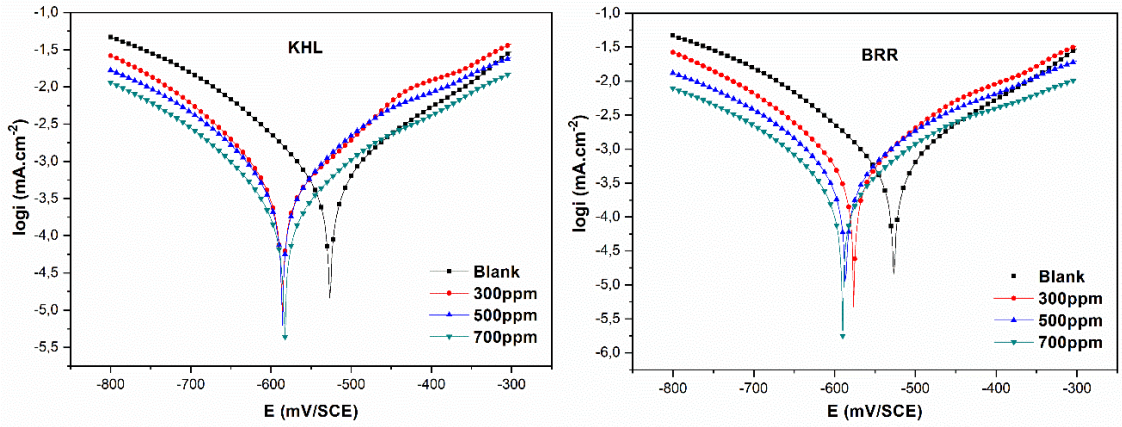

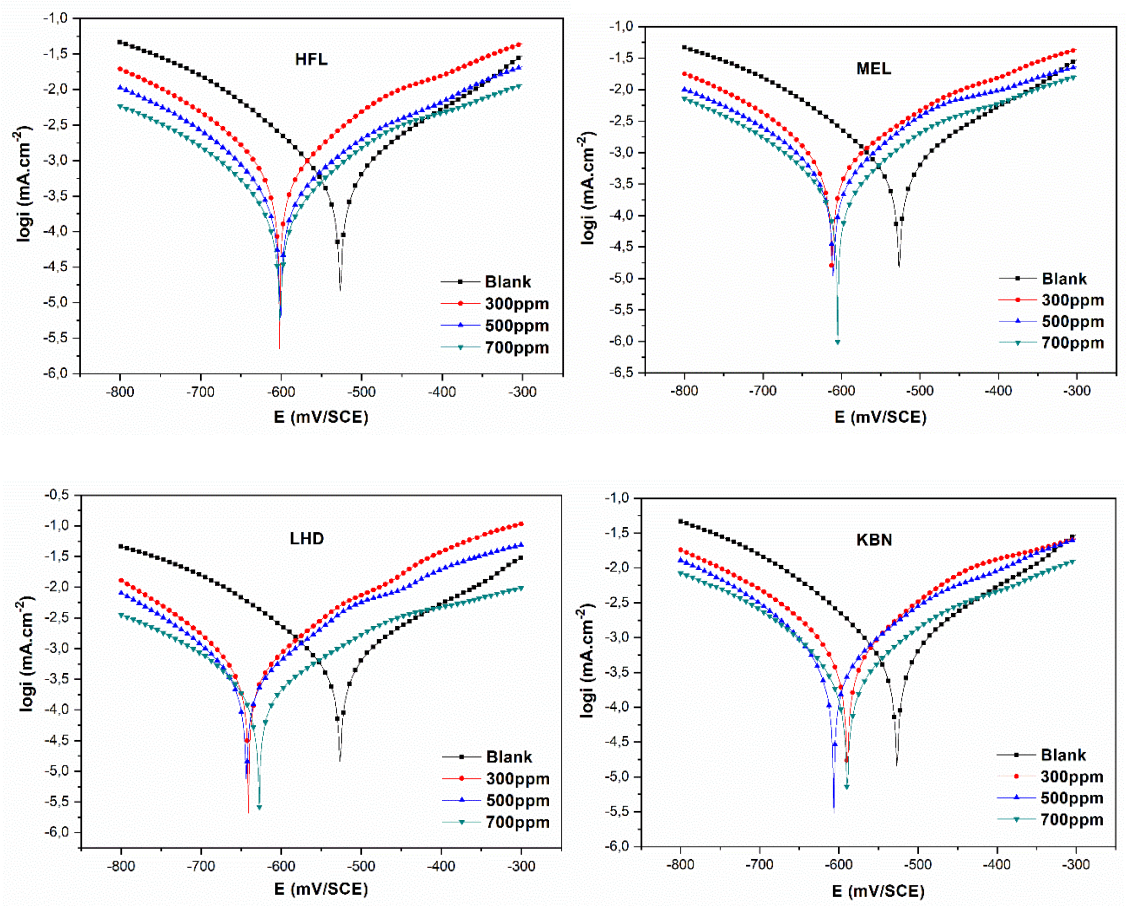

Figure 1. Potentiodynamic polarization plots for mild steel without and with different concentrations of date seeds oil extracts at 298 K.

Table 3. Polarization parameters and the corresponding inhibition efficiency of corrosion of mild steel in 1M HCl containing different concentrations of date seeds oil extracts at 298 K.

	C_{inh} (ppm)	E_{corr} (mV/SCE)	PDP method			*IE%*
			i_{corr}(mA cm^{-2})	β_a(mV dec^{-1})	β_c(mV dec^{-1})	
Blank	-	-531.1	0.3856	93.2	-92.6	-
KHL	300	-590.1	0.1688	57.2	-48.8	56.22
	500	-590.2	0.1238	42.8	-42.0	67.89
	700	-587.4	0.0747	51.3	-46.3	80.62
BRR	300	-580.3	0.1461	41.4	-41.5	62.11
	500	-590.7	0.1117	42.2	-41.7	71.03
	700	-594.5	0.0715	46.3	-42.5	81.45
HFL	300	-606.4	0.1582	32.2	-34.5	58.96
	500	-605.3	0.1256	60.4	-52.2	67.42
	700	-605.9	0.0906	64.0	-58.3	76.48
MEL	300	-616.2	0.2097	46.4	-43.8	45.61
	500	-614.9	0.1378	49.3	-47.3	64.26
	700	-609.2	0.0922	55.0	-51.8	76.08
LHD	300	-645.3	0.1767	55.8	-50.4	54.17
	500	-648.0	0.1406	61.4	-53.8	63.53
	700	-632.4	0.1077	68.5	-58.9	72.06
KBN	300	-593.9	0.1760	44.9	-44.7	54.35
	500	-611.0	0.1418	55.1	-47.1	63.22
	700	-593.7	0.1076	60.7	-54.6	72.09

3.2.2.2. EIS measurements.

In the present investigation, the EIS experiments were performed to study the corrosion processes that occur at the electrode/electrolyte interface without and with inhibitors. Figure 2

shows the electrochemical Nyquist spectra of mild steel in 1M HCl at 298K. From the Nyquist impedance spectra, we observe that the diameters of the capacitive loops increase with the increasing concentrations of date seed oil extracts, which increases the inhibitory efficiency of the examined additives [35,36]. Therefore, the impedance spectra (Figure 2) obtained without and with date seeds oil have a single capacitive loop, suggesting that only one charge transfer process occurred during the dissolution of the metal in the acid medium [37].

An equivalent electrical circuit corresponding to the best impedance data has been introduced in Figure 2. This circuit is composed of a parallel connection between the R_p and C_{dl}, and is connected in series with a solution resistor (R_s). A constant phase element (CPE) was introduced instead of the C_{dl} to achieve a more precise setting because the C_{dl} does not act as an ideal capacitor [38]. The impedance of a CPE has recognized by the expression (8):

$$Z_{CPE} = Y_{\circ}^{-1} (j\omega)^{-n} \quad (8)$$

where $Y_{\circ}$, ω, and j represent the CPE constant, the angular frequency, and the imaginary number, respectively. The n was the phase shift ($-1 \leq n \leq 1$), which demonstrated that CPE could be used as a capacitor (n=1), resistance (n=0), and Inductance (n= -1).

The C_{dl} can be calculated using the following equation (9):

$$C_{dl} = Y_{\circ} (\omega_{max})^{n-1} \quad (9)$$

where $\omega_{max} = 2\pi f_{max}$, f_{max} is the frequency at which the imaginary component of the impedance is maximum.

The electrochemical parameters obtained are given in Table 4. From this table, the R_p values were found to increase proportionally with oil extract concentrations, while the C_{dl} values decreased with the rise of the additive's concentrations. This observation is often interpreted by the coverage of additives on the working electrode surface. Electrochemical results were in perfect conformity with the results obtained from the gravimetric study.

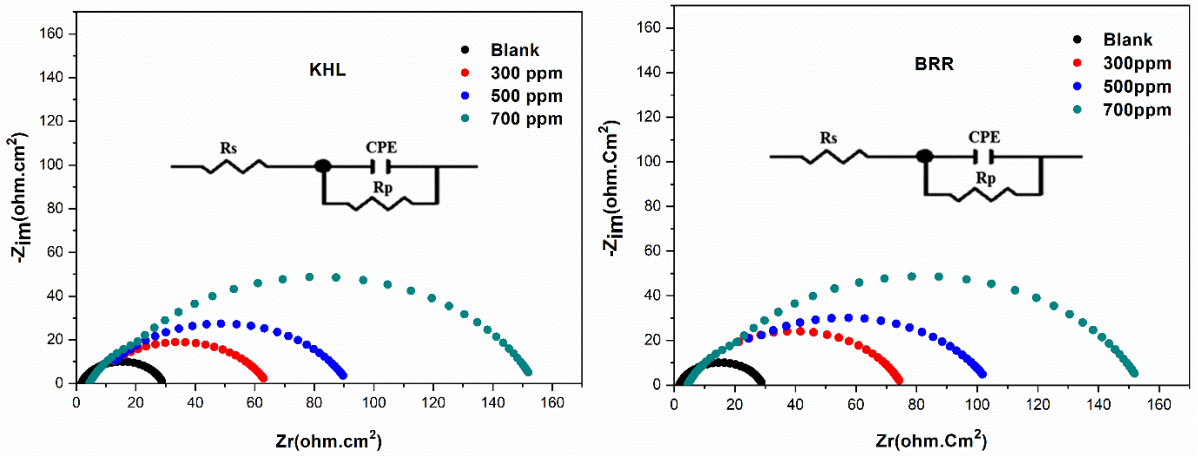

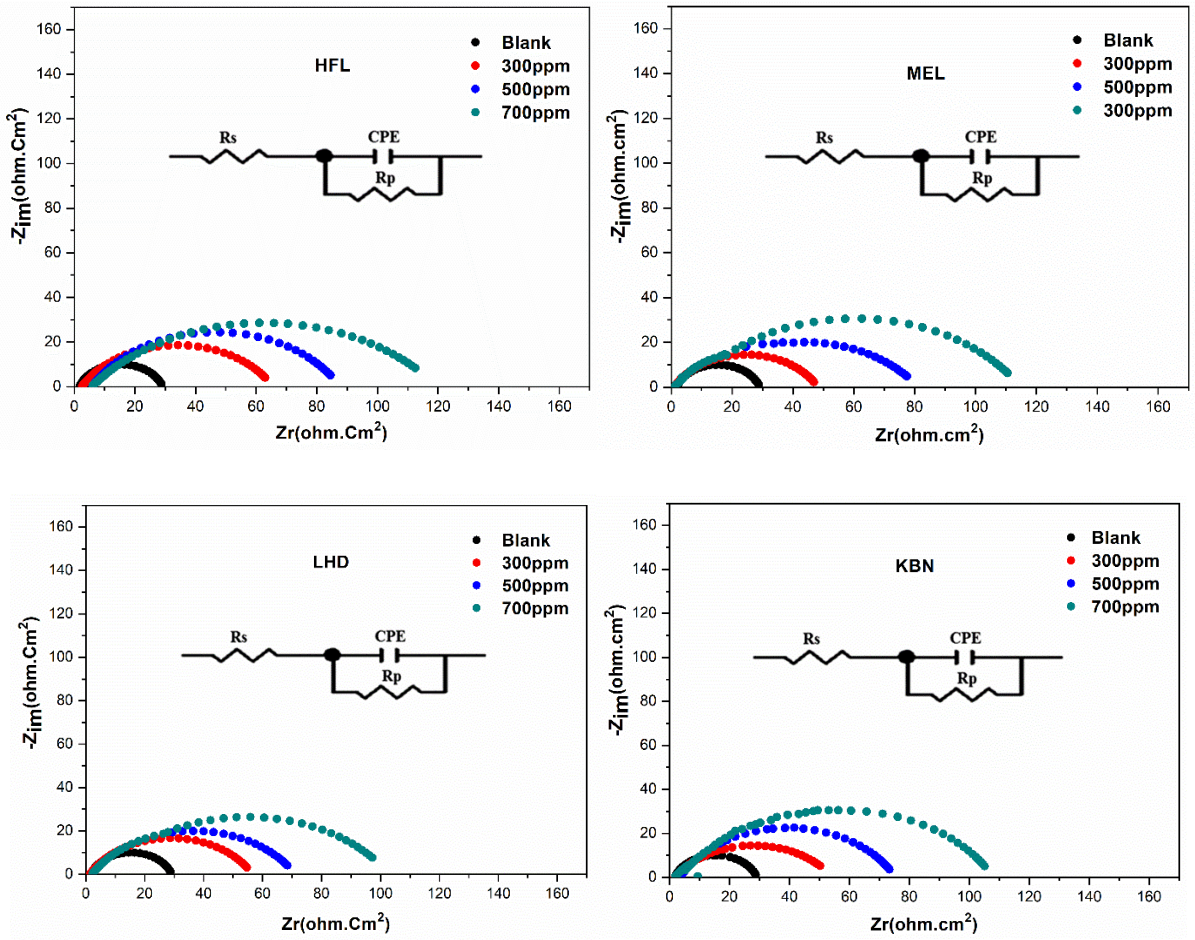

Figure 2. Nyquist diagrams of mild steel immersed in 1 M HCl solution without and with different concentrations of date seeds oil extracts at 298K.

Table 4. Impedance parameters for mild steel samples in the presence and absence of different concentrations of date seeds oil extracts in at 298 K.

	C_{inh} (ppm)	Re (Ω. cm^2)	R_p ($\Omega.cm^2$)	CPE		C_{dl} ($\mu F/cm^2$)	*IE (%)*
				n	($10^{-6}/S^n$. Ω^{-1} . cm^{-2})		
Blank	-	1.764	27.19	0.8030	359.60	113.90	-
KHL	300	5.319	62.11	0.7278	316.27	73.38	56.22
	500	6.581	84.71	0.7291	266.58	65.14	67.90
	700	8.242	140.2	0.7578	169.89	51.52	80.60
BRR	300	4.386	71.79	0.7616	259.28	74.20	62.12
	500	8.743	93.94	0.7157	292.17	70.19	71.05
	700	9.428	144.9	0.7539	202.59	64.03	81.23
HFL	300	2.525	66.12	0.6786	454.30	85.97	58.88
	500	5.862	83.62	0.6853	367.25	74.02	67.48
	700	5.737	116.0	0.591	491.06	67.60	76.56
MEL	300	1.032	49.89	0.7022	447.23	89.02	45.50
	500	6.641	76.02	0.6273	505.22	72.67	64.23
	700	6.295	113.6	0.6536	366.21	67.60	76.07
LHD	300	1.455	59.34	0.6919	476.75	97.53	54.17
	500	2.147	74.44	0.6682	430.30	77.81	63.47
	700	3.039	97.42	0.6396	432.94	72.39	72.08
KBN	300	1.708	59.53	0.6379	637.60	99.64	54.33
	500	2.476	74.03	0.7097	364.66	82.80	63.27
	700	3.216	97.44	0.7003	326.67	74.55	72.09

3.3. Adsorption isotherm.

Generally, the inhibitory effect of a given inhibitor depends on its adsorption capacity on the metal surface by displacing water molecules from a corroding interface [39] (equation (10)):

$$Inh_{sol} + H_2O_{ads} \leftrightarrow Inh_{ads} + H_2O_{sol} \quad (10)$$

where $Inh_{(sol)}$ and $Inh_{(ads)}$ respectively represent the inhibitor in the aqueous solution and the inhibitor adsorbed on the metal surface.

In this context, different models of adsorption isotherms can be used to understand the adsorption process of organic molecules on a metal surface. The data obtained from the weight loss experiments might be fitted by different adsorption isotherm models such as Langmuir, Freundlich, Temkin, and Frumkin. Langmuir isotherm represented the best fit of the experimental data. According to equation (11) [40]:

$$\frac{C_{inh}}{\theta} = \frac{1}{K_{ads}} + C_{inh} \quad (11)$$

where C_{inh} is the inhibitor concentration, θ is the surface coverage, and K_{ads} is the equilibrium constant.

According to Figure 3 and Table 5, the plot of C_{inh}/θ versus C_{inh} characterized by a high correlation coefficient indicates that the examined additives are adsorbed on the mild steel surface according to Langmuir adsorption isotherm. The standard free energy of adsorption ($\Delta G°_{ads}$) was calculated using equation (12) [41,42]:

$$\Delta G°_{ads} = -RT \ln(55.5K_{ads}) \quad (12)$$

where R and T refer respectively to the universal gas constant and absolute temperature. In general, values of free energy adsorption around or less than -20 kJ mol^{-1} correspond to the physical adsorption process (physisorption), while those around or above -40 kJ mol^{-1} reveal that the adsorption is mainly classified as a chemisorptions [43]. The results of this study suggest that the physical adsorption process was found to be a key force in the inhibition mechanism.

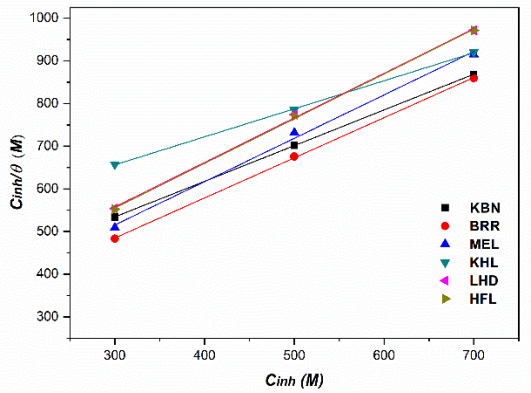

Figure 3. Langmuir isothermal curves for mild steel in 1M HCl containing different concentrations of date seed oil extracts at 298K.

Table 5. Langmuir isotherm parameters for mild steel in 1M HCl solution containing different concentrations of date seed oil extracts at 298K.

Inhibitor's abbreviation	R^2	K_{ads} (M^{-1}) $\times 10^{-3}$	$-\Delta G°_{ads}$(KJ.mol^{-1})
KHL	0.999	3.39	-4.134
BRR	0.999	4.72	-3.315
HFL	0.994	4.68	-3.340
MEL	0.999	2.19	-5.222
LHD	0.998	4.02	-3.716
KBN	0.999	4.04	-3.704

3.4. Surface analysis.

To evaluate the morphology of the steel surface to prove if the inhibition is due to the formation of a film of organic molecules on its surface, we used scanning electron microscopy (SEM). Figure 4 shows SEM images of (a) the polished mild steel specimen, (b) the steel surface after immersion in 1M HCl without inhibitors for 24 h, and the surface of the mild steel after immersion in 1M HCl solution containing 700 ppm of (c) KHL, (d) BRR, (e) HFL, (f) MEL, (g) LHD, and (h) KBN, respectively. The resulting scanning electron microscopies demonstrate that the steel's surface has strongly deteriorated in a corrosive environment (1M HCl) in the absence of the inhibitor because of a corrosion attack. However, after 24 h of immersion in 1M HCl medium at 298K in the presence of 700 ppm of the inhibitors: KHL, BRR, HFL, MEL, LHD, and KBN (Figures. (c), (d), (e), (f), (g), and (h)), it has observed that the surface of the steel has covered with a plaque product reflecting the presence of an organic product. Consequently, all the metallics surfaces are relatively smooth compared to those obtained for blank. Furthermore, EDX spectra (Figures. (a'), (b'), (c'), (d'), (e'), (f'), (g'), and (h')) were performed to confirm the presence of the examined inhibitors on the metal surfaces. The EDX spectra of the mild steel polished (Figs. (a')) had the highest percentage of atomic iron and the lowest atomic carbon content. While the untreated (blank) mild steel surface (Figures. (b')) had the lowest percentage of iron and the highest percentage of atomic oxygen and chlorine. So, this confirmed the formation of corrosion products. However, the EDX spectra of the inhibitor adsorbed on the mild steel surface (Figures. (c'), (d'), (e'), (f'), (g'), and (h')) showed higher intensity of carbon and oxygen peaks, which confirmed the deposition or adsorption of inhibitor molecules on the mild steel surface.

These results indicate that inhibition occurs due to the formation of an adherent, stable and insoluble deposit that prevents access of the electrolyte to the steel surface, which reduces the dissolution of the steel in corrosive media and provides significant prevention against corrosion.

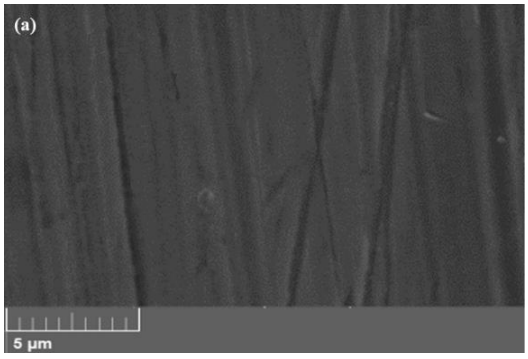

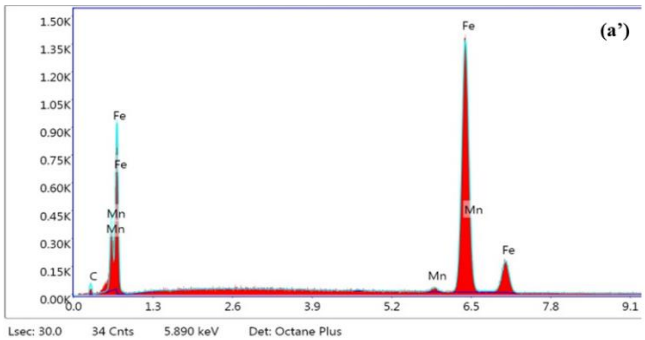

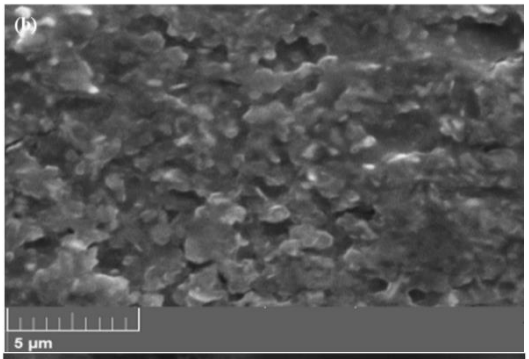
(b)
5 µm

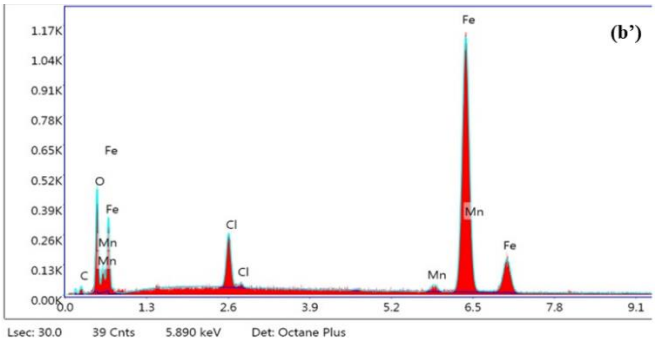
(b')
Fe
O
Fe
Mn
Mn
C
Cl
Cl
Mn
Fe
Lsec: 30.0 39 Cnts 5.890 keV Det: Octane Plus

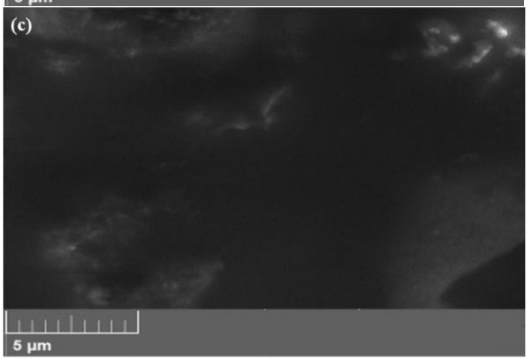
(c)
5 µm

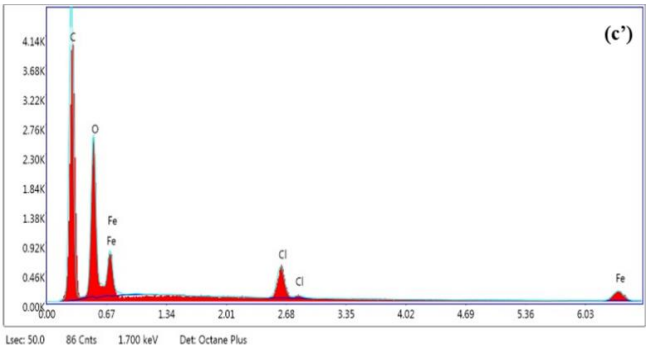
(c')
C
O
Fe
Fe
Cl
Cl
Fe
Lsec: 50.0 86 Cnts 1.700 keV Det: Octane Plus

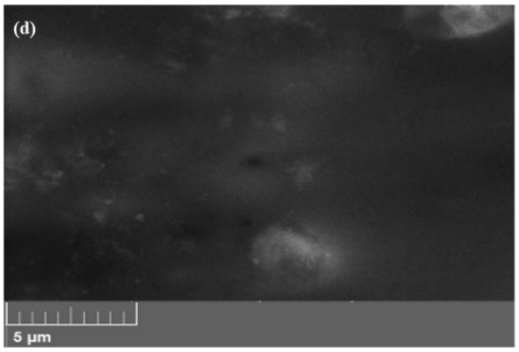
(d)
5 µm

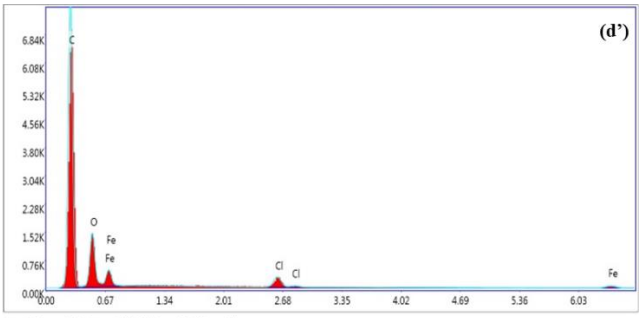
(d')
C
O
Fe
Fe
Cl
Cl
Fe
Lsec: 50.0 76 Cnts 1.550 keV Det: Octane Plus

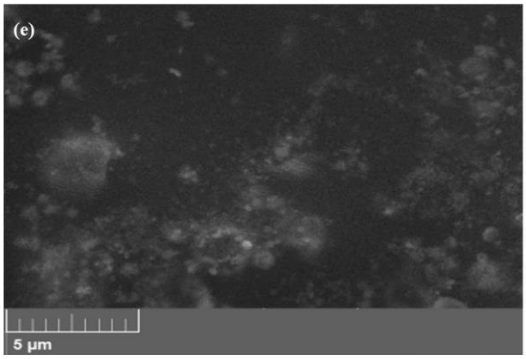
(e)
5 µm

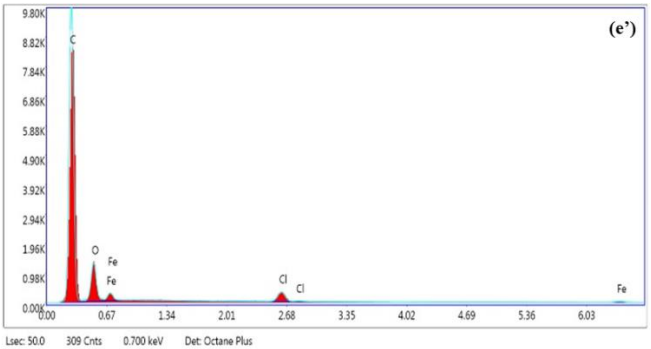
(e')
C
O
Fe
Fe
Cl
Cl
Fe
Lsec: 50.0 309 Cnts 0.700 keV Det: Octane Plus

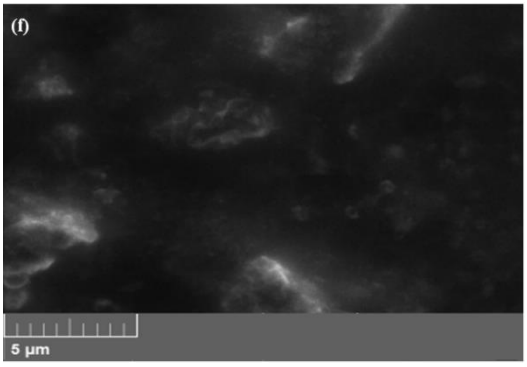
(f)
5 µm

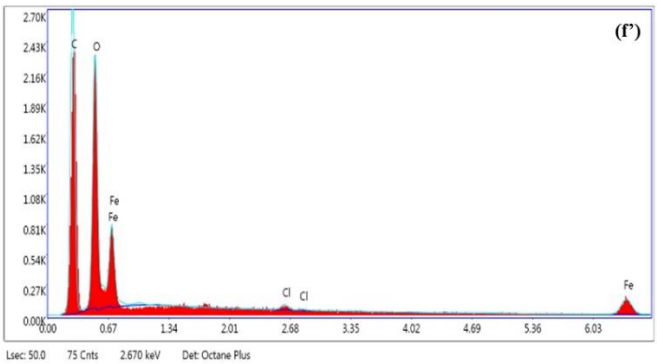
(f')
C
O
Fe
Fe
Cl
Cl
Fe
Lsec: 50.0 75 Cnts 2.670 keV Det: Octane Plus

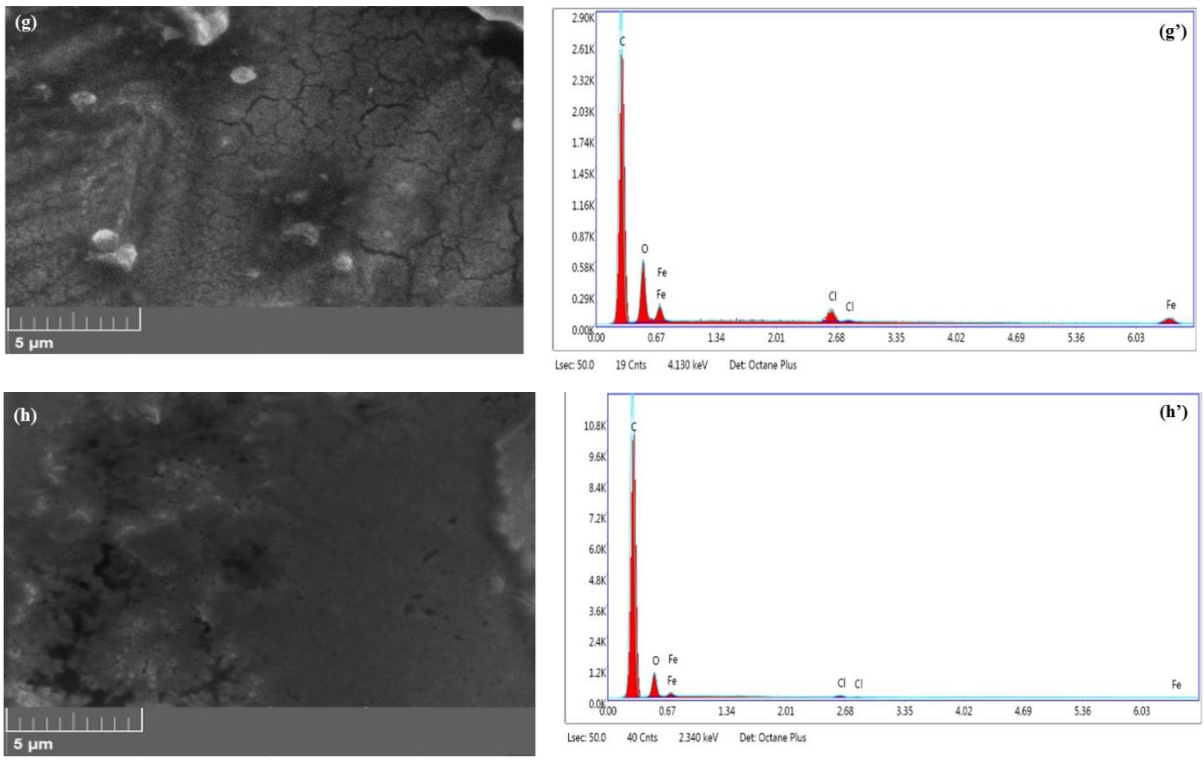

Figure 4. SEM images and EDX spectra of mild steel (**(a);(a'))** alone, (**(b); (b'))** corroded after 24 h of immersion time in a 1 M HCl solution, and **(c)** after immersion with 700 ppm of (**(c); (c'))** BRR (**(d); (d'))** KHL (**(e); (e'))** HFL (**(f); (f'))** MEL (**(g); (g'))** LHD, and (**(h); (h'))** KBN at 298 K.

Therefore, the data achieved here confirm the results of electrochemical measurements and imply that this extract is an effective corrosion inhibitor for the protection of mild steel in 1M HCl solution in the following order BRR > KHL > HFL > MEL > LHD > KBN.

3.5. Quantum chemical calculations.

The gas-liquid chromatography analysis of the prepared Date Seed extracts showed that the dominant unsaturated and saturated fatty acids are oleic acid (46.00% - 50.87%) and lauric acid (10.11% - 19.03%) (Table 1). The quantum parameters of the selected fatty acids were performed to get more light on the inhibition mechanism of these extracts on the surface of the mild steel.

The optimized geometry, Lowest Unoccupied Molecular Orbital (ELUMO), Highest Occupied Molecular Orbital (EHOMO), and Molecular electrostatic potential (MEP) of these fatty acids are shown in Figure 5, as well as the values of the theoretical parameters, ELUMO, EHOMO, ΔE, χ, μ, σ, η, ω, N, and ΔN are presented in Table 6. The higher value of the HOMO energy (EHOMO) for a given molecule indicates its higher ability to donate electrons to an appropriate acceptor having a low-energy empty molecular orbital, while the higher value of ELUMO is associated with the electron-accepting tendency of this molecule. Table 6 shows that for both studied structures (Oleic and Lauric acids), high EHOMO values were obtained for oleic acid, indicating the high ability of this molecule to give electrons to the metal surface (mild steel). On the other hand, the lower values of the gap energy (ΔE) of both fatty acids indicate clearly that these structures also have the capability for high chemical reactivity and molecular softness [39]. Furthermore, the positive values of ΔN, which is lower than 3.6e, suggest the ability of both dominant fatty acids molecules to donate electrons (π and/or lone pair electrons) to the vacant 3d-orbital of the iron surface [40,41]. The lauric acid has a lower dipole moment value, indicating a stronger coating on the metal surface [42]. According to the

literature, a good corrosion inhibitor molecule is characterized by a low electronegativity (χ) [43–45]. From obtained results, we note that the electronegativity values (χ) obtained for both fatty acids indicate the high inhibition efficiency of these fatty acids. Absolute hardness (η) and softness (σ) are fundamental properties for measuring molecular stability and reactivity. The chemical hardness represents the resistance of a molecule to deformation or polarization under small perturbations in a chemical reaction. The obtained results of both selected fatty acids show that these compounds have a similar chemical hardness. To examine the efficiency of the studied extracts, the electrophilicity and nucleophilicity parameters are also investigated to determine the chemical behavior of fatty acids studies [28]. Indeed, the electrophilicity index (ω) indicates the tendency of inhibiting molecules from accepting electrons, while the nucleophilic index (N), measures the electron-donor ability. From the acquired results, it can be observed that oleic acid has a higher value of N and a lower value compared with Lauric acid, indicating thus that oleic acid has a greater tendency to give electrons to the metal surface and have less electron acceptor ability from the metal surface compared to Lauric acid [46]. Also, in Figure 5, the electrostatic potential (MEP) was studied to identify regions on molecules that govern its adsorption on the metal surface. Regions with a strong negative and positive molecular electrostatic potentials surface (MEP) are donor and acceptor sites, respectively [47]. The MEP surface of the selected inhibitors is represented in different colors where the light blue colors stand for the location of nucleophilic attacks while the red, orange, and yellow colors express the region's electrophilic attacks [48]. Indeed, the electrophilic attacks are located around oxygen atoms and some carbon atoms for these fatty acids. These sites are considered to have the greatest ability to donate electrons to the vacant d-orbitals of the metal atoms and, thus, a greater interaction on the metal surface, while; nucleophilic attacks occur around the rest of the carbon atoms for these two green fatty acids. On the other hand, the high amount of light green color shows the neutral region found in the molecules [49]. These regions in the molecules give very valuable information for intermolecular interactions, and the MEP surface reflects the performance of the upcoming groups.

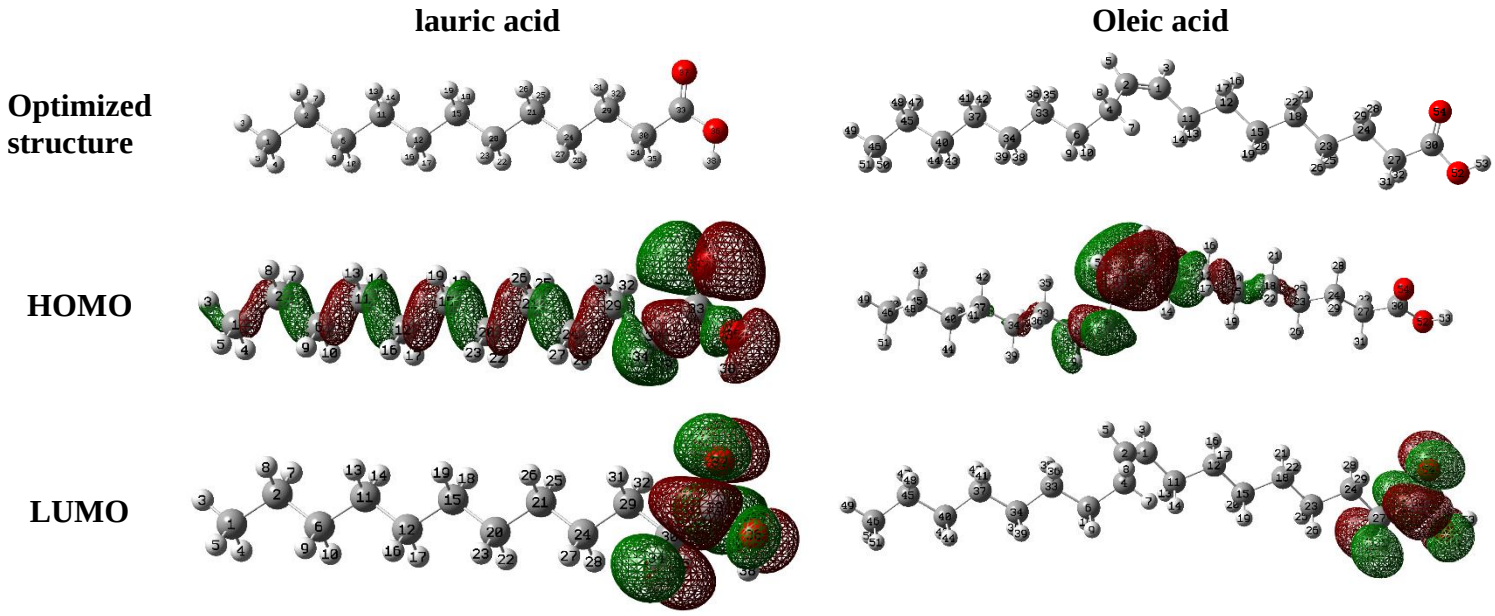

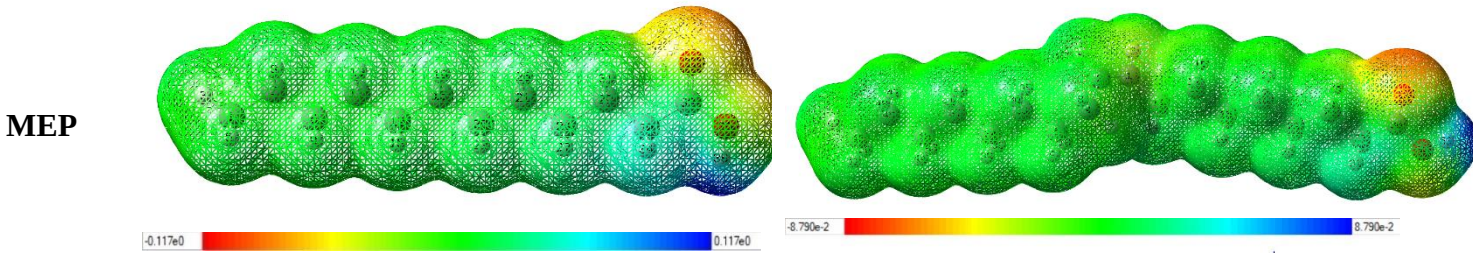

Figure 5. Optimized structures, HOMO, LUMO, and MEP(s) for oleic and lauric fatty acids compounds by DFT calculations at the B3LYP/6-311G(d, p) level.

Table 6. Quantum chemical descriptors of the studied oleic and lauric acids inhibitors calculated at the B3LYP/6-311G (d.p) level of theory.

	E_{HOMO} (eV)	E_{LUMO} (eV)	ΔE(eV)	μ(eV)	X(eV)	η(eV)	σ	ω	N	ΔN
Oleic acid	-6.69691	-0.51816	6.17875	-3.60753	3.60753	3.08937	0.32369	2.10630	2.42025	0.549053
Lauric acid	-7.94620	-0.52849	7.41771	-4.23735	4.23735	3.70885	0.269625	2.42057	1.17096	0.325988

3.6. Corrosion inhibition mechanism.

The adsorption mechanism of the investigated additives on the mild steel surface is proposed, as shown in Figure 6. This figure describes how the inhibitory molecules present in the date seed oil extracts could adsorb on the surface of the steel and prevent it from corrosion [43]. The gas-liquid chromatographic analysis shows that date seed oil extracts contain mainly oleic acid (46.00% - 50.87%) and lauric acid (10.11% - 19.03%), along with other fatty acids have also been identified. However, these acids contain oxygen atoms in functional groups (COOH), which meets the general consideration of the typical corrosion inhibitors. Consequently, it can be seen that the adsorption of these acids takes place by a strong attraction between the partially negatively charged carboxyl group of the inhibitor molecule and the positively charged (oxidized) metal surface [39,50,51]. The increase in the inhibition efficiency of date seed oil extracts indicates that the inhibition mechanism involves the formation of a protective film on the metal surface [39,52].

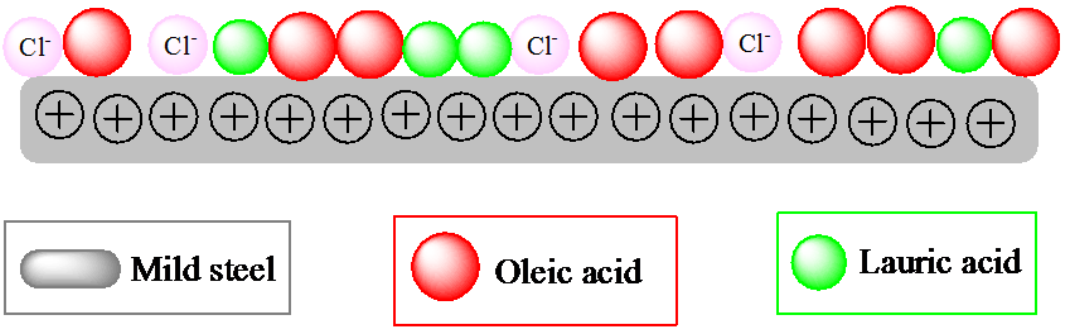

Figure 6. Schematic model of the adsorption mechanism of oleic and lauric acids on the mild steel surface in 1M HCl.

4. Conclusions

This study examined the corrosion inhibition effect of six "date seed" extracts for mild steel in 1 M HCl solution. This effect was evaluated using weight loss and electrochemical measurements and has complemented by surface analysis of polished and corroded steel samples immersed in uninhibited and inhibited solutions with SEM and EDX analysis. Based on the overall experimental results obtained, we can deduce that all six date seed oil extracts have good corrosion inhibition properties of mild steel in a 1M hydrochloric medium. The

inhibition efficiency increases with increasing the additive concentration following the order: KBN (72.05%) < LHD (72.08%) < MEL (76.07%) < HFL (76.48%) < KHL (80.61%) < BRR (81.46%) with the optimum extract concentration (700 ppm) studied. The inhibitory efficiencies obtained by PDP, EIS technics, and weight loss measurements agree. Further, the polarization data indicated that the examined additives were considered cathodic rather than anodic inhibitors. In addition, the adsorption of useful compounds on the mild steel surface obeyed a Langmuir isotherm. Surface characterization techniques (SEM and EDX) confirm the existence of a protective layer on the metal surface, which reduces the corrosion rate of MS in 1M HCl. DFT calculations indicate that these organic extracts containing a higher percentage of Oleic and Lauric fatty acids have strongly adsorbed on the Fe surface, which results in better inhibitory efficiency. The results obtained from experimental and theoretical measurements are in good agreement.

Funding

This research received no external funding.

Acknowledgments

Cadi Ayyad University (UCA), especially the Center of Analysis and Characterization (CAC) of the Faculty of Sciences Semlalia in Marrakech, are gratefully acknowledged for their generous support.

Conflicts of Interest

The authors declare no conflict of interest.

References

1. Loto, R. T. Corrosion Inhibition Studies of the Combined Admixture of 1, 3-Diphenyl-2-Thiourea and 4-Hydroxy-3-Methoxybenzaldehyde on Mild Steel in Dilute Acid Media. *Revista Colombiana de Química* **2017**, *46*, 20–32, http://dx.doi.org/10.15446/rev.colomb.quim.v1n1.59578.
2. Murmu, M.; Saha, S. Kr.; Murmu, N. C.; *et al*. Effect of Stereochemical Conformation into the Corrosion Inhibitive Behaviour of Double Azomethine Based Schiff Bases on Mild Steel Surface in 1 Mol L−1 HCl Medium: An Experimental, Density Functional Theory and Molecular Dynamics Simulation Study. *Corrosion Science* **2019**, *146*, 134–151, https://doi.org/10.1016/j.corsci.2018.10.002.
3. Lgaz, H.; Salghi, R.; Chaouiki, A.; *et al*. Pyrazoline Derivatives as Possible Corrosion Inhibitors for Mild Steel in Acidic Media: A Combined Experimental and Theoretical Approach. *Cogent Engineering* **2018**, *5*, 1441585, https://doi.org/10.1080/23311916.2018.1441585.
4. Hrimla, M.; Bahsis, L.; Laamari, M. R.; *et al*. An Overview on the Performance of 1,2,3-Triazole Derivatives as Corrosion Inhibitors for Metal Surfaces. *International Journal of Molecular Sciences* **2022**, *23*, 16, https://doi.org/10.3390/ijms23010016.
5. Alamri, A. H. Localized Corrosion and Mitigation Approach of Steel Materials Used in Oil and Gas Pipelines – An Overview. *Engineering Failure Analysis* **2020**, *116*, 104735, https://doi.org/10.1016/j.engfailanal.2020.104735.
6. Abdel-Rahman, I.; Elmsellem, H.; Yousfi, F.; *et al*. Eco-Friendly Chamaerops Humilis L. Fruit Extract Corrosion Inhibitor for Mild Steel in 1 M HCl. **2020**, *9*, 446–459, https://doi.org/10.17675/2305-6894-2020-9-2-4.
7. Emregül, K. C.; Hayvalí, M. Studies on the Effect of a Newly Synthesized Schiff Base Compound from Phenazone and Vanillin on the Corrosion of Steel in 2M HCl. *Corrosion Science* **2006**, *48*, 797–812, https://doi.org/10.1016/j.corsci.2005.03.001.
8. Moretti, G.; Guidi, F.; Fabris, F. Corrosion Inhibition of the Mild Steel in 0.5M HCl by 2-Butyl-Hexahydropyrrolo[1,2-b][1,2]Oxazole. *Corrosion Science* **2013**, *76*, 206–218, https://doi.org/10.1016/j.corsci.2013.06.044.

9. Stupnišek-Lisac, E.; Gazivoda, A.; Madžarac, M. Evaluation of Non-Toxic Corrosion Inhibitors for Copper in Sulphuric Acid. *Electrochimica Acta* **2002**, *47*, 4189–4194, https://doi.org/10.1016/S0013-4686(02)00436-X.
10. Bouyanzer, A.; Hammouti, B.; Majidi, L. Pennyroyal Oil from Mentha Pulegium as Corrosion Inhibitor for Steel in 1M HCl. *Materials Letters* **2006**, *60*, 2840–2843, https://doi.org/10.1016/j.matlet.2006.01.103.
11. Dewangan, A. K.; Dewangan, Y.; Verma, D. K.; *et al.* 4 - Synthetic Environment-Friendly Corrosion Inhibitors. In *Environmentally Sustainable Corrosion Inhibitors*; Hussain, C. M.; Verma, C.; Aslam, J., Eds.; Elsevier, **2022**, 71–95, https://www.sciencedirect.com/science/article/pii/B9780323854054000203.
12. Sanaei, Z.; Ramezanzadeh, M.; Bahlakeh, G.; *et al.* Use of Rosa Canina Fruit Extract as a Green Corrosion Inhibitor for Mild Steel in 1M HCl Solution: A Complementary Experimental, Molecular Dynamics and Quantum Mechanics Investigation. *Journal of Industrial and Engineering Chemistry* **2019**, *69*, 18–31, https://doi.org/10.1016/j.jiec.2018.09.013.
13. Effect of Corrosion on Crude Oil and Natural Gas Pipeline with Emphasis on Prevention by Ecofriendly Corrosion Inhibitors: A Comprehensive Review | SpringerLink https://link.springer.com/article/10.1007/s40735-019-0225-9 (accessed Feb 28, 2022).
14. Popoola, L. T. Organic Green Corrosion Inhibitors (OGCIs): A Critical Review. *Corrosion Reviews* **2019**, *37*, 71–102, https://doi.org/10.1515/corrrev-2018-0058.
15. Argyropoulos, V.; Boyatzis, S. C.; Giannoulaki, M.; *et al.* Organic Green Corrosion Inhibitors Derived from Natural and/or Biological Sources for Conservation of Metals Cultural Heritage. In *Microorganisms in the Deterioration and Preservation of Cultural Heritage*; Joseph, E., Ed.; Springer International Publishing: Cham **2021**, 341–367, https://doi.org/10.1007/978-3-030-69411-1_15.
16. Abdelaziz, S.; Benamira, M.; Messaadia, L.; *et al*. Green Corrosion Inhibition of Mild Steel in HCl Medium Using Leaves Extract of Arbutus Unedo L. Plant: An Experimental and Computational Approach. *Colloids and Surfaces A: Physicochemical and Engineering Aspects* **2021**, *619*, 126496, https://doi.org/10.1016/j.colsurfa.2021.126496.
17. Deyab, M. A.; Mohsen, Q.; Guo, L. Aesculus Hippocastanum Seeds Extract as Eco-Friendly Corrosion Inhibitor for Desalination Plants: Experimental and Theoretical Studies. *Journal of Molecular Liquids* **2022**, *361*, 119594, https://doi.org/10.1016/j.molliq.2022.119594.
18. Umoren, S. A.; Gasem, Z. M.; Obot, I. B. Natural Products for Material Protection: Inhibition of Mild Steel Corrosion by Date Palm Seed Extracts in Acidic Media. *Ind. Eng. Chem. Res.* **2013**, *52*, 14855–14865, https://doi.org/10.1021/ie401737u.
19. Gerengi, H.; Sahin, H. I. Schinopsis Lorentzii Extract As a Green Corrosion Inhibitor for Low Carbon Steel in 1 M HCl Solution. *Ind. Eng. Chem. Res.* **2012**, *51*, 780–787, https://doi.org/10.1021/ie201776q.
20. Alahyane, A.; Harrak, H.; Elateri, I.; *et al.* Evaluation of Some Nutritional Quality Criteria of Seventeen Moroccan Dates Varieties and Clones, Fruits of Date Palm (*Phoenix Dactylifera* L.). *Braz. J. Biol.* **2021**, *82*, https://doi.org/10.1590/1519-6984.236471.
21. Alahyane, A.; Harrak, H.; Ayour, J.; *et al*. Bioactive Compounds and Antioxidant Activity of Seventeen Moroccan Date Varieties and Clones (Phoenix Dactylifera L.). *South African Journal of Botany* **2019**, *121*, 402–409, https://doi.org/10.1016/j.sajb.2018.12.004.
22. Hrimla, M.; Bahsis, L.; Boutouil, A.; *et al.* Corrosion Inhibition Performance of a Structurally Well-Defined 1,2,3-Triazole Derivative on Mild Steel-Hydrochloric Acid Interface. *Journal of Molecular Structure* **2021**, *1231*, 129895, https://doi.org/10.1016/j.molstruc.2021.129895.
23. Eddy, N. O.; Odoemelam, S. A.; Ogoko, E. C.; *et al*. Experimental and Quantum Chemical Studies of Synergistic Enhancement of the Corrosion Inhibition Efficiency of Ethanol Extract of Carica Papaya Peel for Aluminum in Solution of HCl. *Results in Chemistry* **2022**, *4*, 100290, https://doi.org/10.1016/j.rechem.2022.100290.
24. Hrimla, M.; Achour, Y.; Bahsis, L.; *et al*. Systematic Investigation of the Adsorption and Inhibition Properties of a New Clickable 1,2,3-Triazole Compound for Mild Steel in 1 M HCl Medium. *ChemistrySelect* **2021**, *6*, 12895–12913, https://doi.org/10.1002/slct.202102871.
25. Abdallah, M.; Soliman, K. A.; Alfattani, R.; *et al*. Insight of Corrosion Mitigation Performance of SABIC Iron in 0.5 M HCl Solution by Tryptophan and Histidine: Experimental and Computational Approaches. *International Journal of Hydrogen Energy* **2022**, *47*, 12782–12797, https://doi.org/10.1016/j.ijhydene.2022.02.007.
26. Munawaroh, H. S. H.; Sunarya, Y.; Anwar, B.; *et al*. Protoporphyrin Extracted from Biomass Waste as Sustainable Corrosion Inhibitors of T22 Carbon Steel in Acidic Environments. *Sustainability* **2022**, *14*, 3622, https://doi.org/10.3390/su14063622.
27. Corrosion Resistance and Forming Mechanism of the Lauric Acid/Graphene Composite Films on Aluminum Alloy by Electrodeposition - Li - **2021** - Advanced Engineering Materials - Wiley Online Library https://onlinelibrary.wiley.com/doi/abs/10.1002/adem.202001540 (accessed Jul 12, 2022).
28. Al-Amiery, A. A.; Mohamad, A. B.; Kadhum, A. A. H.; *et al.* Experimental and Theoretical Study on the Corrosion Inhibition of Mild Steel by Nonanedioic Acid Derivative in Hydrochloric Acid Solution. *Sci Rep* **2022**, *12*, 4705, https://doi.org/10.1038/s41598-022-08146-8.

29. Devshony, S.; Eteshola, E.; Shani, A. Characteristics and Some Potential Applications of Date Palm (Phoenix Dactylifera L.) Seeds and Seed Oil. *Journal of the American Oil Chemists' Society* **1992**, *69*, 595–597, https://doi.org/10.1007/BF02636115.
30. Al-Shahib, W.; Marshall, R. J. Fatty Acid Content of the Seeds from 14 Varieties of Date Palm Phoenix Dactylifera L. *International Journal of Food Science & Technology* **2003**, *38*, 709–712, https://doi.org/10.1046/j.1365-2621.2003.00723.x.
31. Besbes, S.; Blecker, C.; Deroanne, C.; *et al.* Date Seeds: Chemical Composition and Characteristic Profiles of the Lipid Fraction. *Food Chemistry* **2004**, *84*, 577–584, https://doi.org/10.1016/S0308-8146(03)00281-4.
32. Adekunle, A. S.; Olasunkanmi, L. O.; Durodola, S. S.; *et al*. Investigation on corrosion inhibition of mild steel by extract of Dracaena arborea leaves in acidic medium. *Chemistry Africa* **2021**, 4(3), 647-658, https://doi.org/10.1007/s42250-021-00246-8.
33. Ricky, E. X.; Mpelwa, M.; Xu, X. The study of m-pentadecylphenol on the inhibition of mild steel corrosion in 1 M HCl solution. *Journal of Industrial and Engineering Chemistry* **2021**, 101, 359-371, https://doi.org/10.1016/j.jiec.2021.05.047.
34. Ali, E. H.; Himdan, T. A.; Ahmed, Z. W. Gallic Acid as Corrosion Inhibitor for Aluminum 6061 in Alkali Solutions. *Ibn AL- Haitham Journal For Pure and Applied Sciences* **2019**, *32*, 17–27, https://doi.org/10.30526/32.1.1983.
35. Pal, S.; Lgaz, H.; Tiwari, P.; *et al*. Experimental and Theoretical Investigation of Aqueous and Methanolic Extracts of Prunus Dulcis Peels as Green Corrosion Inhibitors of Mild Steel in Aggressive Chloride Media. *Journal of Molecular Liquids* **2019**, *276*, 347–361, , https://doi.org/10.1016/j.molliq.2018.11.099.
36. Song, Y.; Shan, D.; Han, E.-H. Pitting Corrosion of a Rare Earth Mg Alloy GW93. *Journal of Materials Science & Technology* **2017**, *33*, 954–960, https://doi.org/10.1016/j.jmst.2017.01.014.
37. Coelho, L. B.; Cossement, D.; Olivier, M.-G. Benzotriazole and Cerium Chloride as Corrosion Inhibitors for AA2024-T3: An EIS Investigation Supported by SVET and ToF-SIMS Analysis. *Corrosion Science* **2018**, *130*, 177–189, https://doi.org/10.1016/j.corsci.2017.11.004.
38. Abdallah, M.; A. Hegazy, M.; Ahmed, H.; *et al*. Appraisal of Synthetic Cationic Gemini Surfactants as Highly Efficient Inhibitors for Carbon Steel in the Acidization of Oil and Gas Wells: An Experimental and Computational Approach. *RSC Advances* **2022**, *12*, 17050–17064, https://doi.org/10.1039/D2RA02603A.
39. Hermoso-Diaz, I. A.; Foroozan, A. E.; Flores-De los Rios, J. P.; *et al*. Electrochemical and Quantum Chemical Assessment of Linoleic Acid as a Corrosion Inhibitor for Carbon Steel in Sulfuric Acid Solution. *Journal of Molecular Structure* **2019**, *1197*, 535–546, https://doi.org/10.1016/j.molstruc.2019.07.085.
40. Hrimla, M.; Bahsis, L.; Boutouil, A.; *et al.* A Combined Computational and Experimental Study on the Mild Steel Corrosion Inhibition in Hydrochloric Acid by New Multifunctional Phosphonic Acid Containing 1,2,3-Triazoles. *Journal of Adhesion Science and Technology* **2020**, *34*, 1741–1773, https://doi.org/10.1080/01694243.2020.1728177.
41. Fernandes, C. M.; Alvarez, L. X.; dos Santos, N. E.; *et al*. Green Synthesis of 1-Benzyl-4-Phenyl-1H-1,2,3-Triazole, Its Application as Corrosion Inhibitor for Mild Steel in Acidic Medium and New Approach of Classical Electrochemical Analyses. *Corrosion Science* **2019**, *149*, 185–194, https://doi.org/10.1016/j.corsci.2019.01.019.
42. Umoren, S. A.; Solomon, M. M.; Obot, I. B.; *et al*. Comparative Studies on the Corrosion Inhibition Efficacy of Ethanolic Extracts of Date Palm Leaves and Seeds on Carbon Steel Corrosion in 15% HCl Solution. *Journal of Adhesion Science and Technology* **2018**, *32*, 1934–1951, https://doi.org/10.1080/01694243.2018.1455797.
43. Vinutha, M. R.; Venkatesha, T. V. Review on Mechanistic Action of Inhibitors on Steel Corrosion in Acidic Media: *Port. Electrochim. Acta* **2016**, *34*, 157–184, https://doi.org/10.4152/pea.201603157.
44. Li, X. L.; Xie, B.; Feng, J. S.; *et al.* 2-Pyridinecarboxaldehyde-based Schiff base as an effective corrosion inhibitor for mild steel in HCl medium: Experimental and computational studies. *Journal of Molecular Liquids* **2022**, *345*, 117032, https://doi.org/10.1016/j.molliq.2021.117032.
45. Kokalj, A. Molecular Modeling of Organic Corrosion Inhibitors: Calculations, Pitfalls, and Conceptualization of Molecule–Surface Bonding. *Corrosion Science* **2021**, *193*, 109650, https://doi.org/10.1016/j.corsci.2021.109650.
46. Luo, X.; Dong, C.; Xi, Y.; *et al*. Computational Simulation and Efficient Evaluation on Corrosion Inhibitors for Electrochemical Etching on Aluminum Foil. *Corrosion Science* **2021**, *187*, 109492, https://doi.org/10.1016/j.corsci.2021.109492.
47. Soraya, N.; Rayenne, D.; Boulanouar, M.; *et al.* Structure-Corrosion Inhibition Performance Relationship: Application to Some Natural Free Acids and Antioxidants: *Port. Electrochim. Acta* **2018**, *36*, 23–34, https://doi.org/10.4152/pea.201801023.
48. Mishra, A.; Verma, C.; Lgaz, H.; *et al*. Synthesis, Characterization and Corrosion Inhibition Studies of N-Phenyl-Benzamides on the Acidic Corrosion of Mild Steel: Experimental and Computational Studies. *Journal of Molecular Liquids* **2018**, *251*, 317–332, https://doi.org/10.1016/j.molliq.2017.12.011.
49. Ahmed, S. K.; Ali, W. B.; Khadom, A. A. Synthesis and Investigations of Heterocyclic Compounds as Corrosion Inhibitors for Mild Steel in Hydrochloric Acid. *Int J Ind Chem* **2019**, *10*, 159–173, https://doi.org/10.1007/s40090-019-0181-8.

50. Jayakumar, S.; Nandakumar, T.; Vadivel, M.; *et al*. Corrosion Inhibition of Mild Steel in 1 M HCl Using Tamarindus Indica Extract: Electrochemical, Surface and Spectroscopic Studies. *Journal of Adhesion Science and Technology* **2020**, *34*, 713–743, https://doi.org/10.1080/01694243.2019.1681156.
51. Abdulmajid, A.; Hamidon, T. S.; Rahim, A. A.; *et al*. Tamarind Shell Tannin Extracts as Green Corrosion Inhibitors of Mild Steel in Hydrochloric Acid Medium. *Mater. Res. Express* **2019**, *6*, 106579, https://doi.org/10.1088/2053-1591/ab3b87.
52. Şahin, E. A.; Solmaz, R.; Gecibesler, \ Ibrahim Halil; *et al*. Adsorption Ability, Stability and Corrosion Inhibition Mechanism of Phoenix Dactylifera Extrat on Mild Steel. *Mater. Res. Express* **2020**, *7*, 016585, https://doi.org/10.1088/2053-1591/ab6ad3.